Neuron
Article

Impaired Spatial Representation in CA1 after Lesion of Direct Input from Entorhinal Cortex

Vegard Heimly Brun,[1] Stefan Leutgeb,[1] Hui-Qiu Wu,[2] Robert Schwarcz,[2] Menno P. Witter,[1,3] Edvard I. Moser,[1,*] and May-Britt Moser[1]
[1]Kavli Institute for Systems Neuroscience and Centre for the Biology of Memory, Norwegian University of Science and Technology, 7489 Trondheim, Norway
[2]Maryland Psychiatric Research Center, University of Maryland School of Medicine, Baltimore, MD 21228, USA
[3]Research Institute Neurosciences, Department of Anatomy and Neurosciences, VU University Medical Center, 1007 MB Amsterdam, The Netherlands
*Correspondence: edvard.moser@ntnu.no
DOI 10.1016/j.neuron.2007.11.034

SUMMARY

Place-specific firing in the hippocampus is determined by path integration-based spatial representations in the grid-cell network of the medial entorhinal cortex. Output from this network is conveyed directly to CA1 of the hippocampus by projections from principal neurons in layer III, but also indirectly by axons from layer II to the dentate gyrus and CA3. The direct pathway is sufficient for spatial firing in CA1, but it is not known whether similar firing can also be supported by the input from CA3. To test this possibility, we made selective lesions in layer III of medial entorhinal cortex by local infusion of the neurotoxin γ-acetylenic GABA. Firing fields in CA1 became larger and more dispersed after cell loss in layer III, whereas CA3 cells, which receive layer II input, still had sharp firing fields. Thus, the direct projection is necessary for precise spatial firing in the CA1 place cell population.

INTRODUCTION

Spatial navigation depends on a widespread hippocampal and parahippocampal neural network that includes place cells (O'Keefe and Dostrovsky, 1971), head-direction cells (Taube et al., 1990), and grid cells (Hafting et al., 2005). Hippocampal place cells fire only when the animal is in a certain location in the spatial environment. Their firing fields are thought to reflect the integration of convergent input from entorhinal grid cells, whose firing locations form regularly spaced repetitive grid-like patterns that each tile the entire environment explored by the animal (Hafting et al., 2005). The spacing of the grid fields increases topographically along the dorsoventral axis of the medial entorhinal cortex (MEC) (Fyhn et al., 2004; T. Solstad et al., 2007, Soc. Neurosci., abstract). Because most hippocampal neurons receive input from at least one-quarter of this axis (Amaral and Witter, 1989; Dolorfo and Amaral, 1998), they are likely to integrate spike activity across a broad range of grid scales. Such integration would result in nonrepetitive firing fields within most conventionally sized environments, similar to the fields of typical hippocampal place cells (Fuhs and Touretzky, 2006; McNaughton et al., 2006; O'Keefe and Burgess, 2005; Solstad et al., 2006).

While we are beginning to understand how space is represented in cell assemblies of the entorhinal cortex, it has not been determined how the spatial information is conveyed from entorhinal grid cells to hippocampal place cells. In each subfield of the hippocampal region, place-modulated neurons receive direct inputs from projection neurons in the superficial layers of MEC; axons from layer II cells terminate in the dentate gyrus and CA3 whereas axons from layer III cells terminate in CA1 and subiculum (Witter and Amaral, 2004; Figure 1). Thus, entorhinal grid cells are likely to contact place cells in CA1 directly as well as indirectly through spatially tuned cells in the dentate gyrus and CA3. Previous studies have shown that the direct pathway is sufficient for spatial firing in CA1. Localized firing is maintained after selective disruption of all input from CA3 (Brun et al., 2002) as well as after reduced transmission through the indirect pathway by selective lesions of the dentate gyrus (McNaughton et al., 1989) or by attenuation of firing in CA3 after inactivation of the medial septum (Mizumori et al., 1989). However, these results do not rule out that place fields can be formed by the indirect pathway too, independently of the direct perforant-path input. Principal neurons in both the dentate gyrus and CA3 have strongly localized firing patterns that might be conveyed further to CA1 (Barnes et al., 1990; Fyhn et al., 2004; Leutgeb et al., 2007; Leutgeb et al., 2004). Synaptic plasticity in CA3 is critical for the fast formation of localized firing fields in CA1 when animals explore a novel environment (Nakazawa et al., 2003), and with prolonged training, changes in ensemble representations in CA3 are succeeded by similar changes in CA1 (Leutgeb et al., 2005a), suggesting that CA3 exerts an important influence on the distribution of firing locations in the CA1 population. This influence may mediate the output of pattern completion mechanisms in the associative network of CA3 (Lee et al., 2004; Nakazawa et al., 2002; Vazdarjanova and Guzowski, 2004), which could have a role in generating spatial representations of familiar

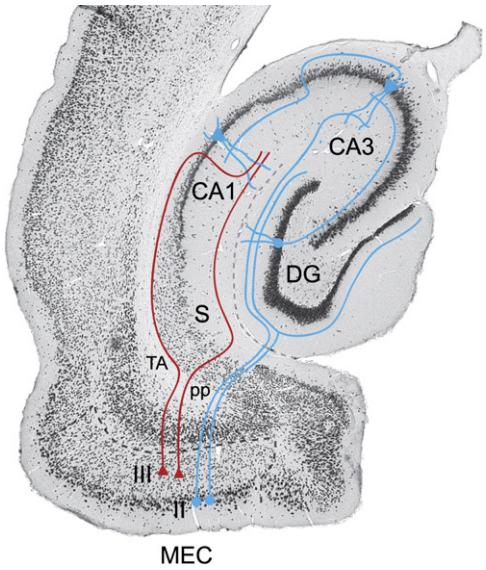

Figure 1. Schematic View of the Direct Input (Red) from Layer III in Entorhinal Cortex to CA1, and the Indirect Input (Blue) from Layer II via the Dentate Gyrus (DG) and CA3

Both perforant-path (pp) and temporoammonic-tract (TA) axons are depicted. S, subiculum; MEC, medial entorhinal cortex with layers II and III labeled. The hippocampal fissure, the lamina dissecans (layer IV) of the entorhinal cortex, and the lateral and medial borders of the MEC are indicated with stippled lines. Connections with the subiculum have not been included.

environments in CA1 independently of the specific momentary sensory inputs (Leutgeb et al., 2005a).

To test specifically whether the direct perforant-path input is necessary for place representation in CA1, we measured spatial modulation of firing in CA1 and CA3 pyramidal cells after selective removal of the direct axonal input from layer III of the entorhinal cortex. We made use of the previously reported observation that local application of the neurotoxin γ-acetylenic GABA (GAG) produces selective lesions in layer III of MEC (Wu and Schwarcz, 1998). The infusions were made unilaterally because the contralateral projections from layer III to CA1 are weak (Witter and Amaral, 2004). The procedure causes extensive cell loss across the entire central portion of the ipsilateral MEC, with variable additional damage to more dorsal and ventral parts of this brain region. Layer II projections to the dentate gyrus and CA3 are left almost intact.

RESULTS

Recording Position in Hippocampal Area CA1

Projections from MEC to CA1 exhibit a more restricted topographical organization than the projections to other subfields of the hippocampal formation (Naber et al., 2001). Because the cell loss after GAG infusions is most profound in the ventromedial-to-intermediate part of the MEC (Wu and Schwarcz, 1998), we expected a more extensive disruption of direct entorhinal input in the ventral-to-intermediate portion of CA1 than in more dorsal areas and a stronger effect in the proximal CA1 (close to CA2) than in the distal part (close to subiculum). The tetrodes were therefore implanted in the proximal part of CA1 at an intermediate septotemporal level, sufficiently ventral to reach the target field of the projections from the lesioned area and sufficiently dorsal to enable us to see spatial modulation of pyramidal cell firing within conventionally sized recording environments (Jung et al., 1994; K.B. Kjelstrup et al., 2007, Soc. Neurosci., abstract). The connectivity between the recording area and the lesion site was verified by unilateral injections of the retrogradely transported tracer Fluorogold at the coordinates used for unit recording in CA1 (Figure 2, top panels). The injections were placed close to the hippocampal fissure to label the terminal fields of entorhinal fibers in stratum lacunosum-moleculare. As shown in Figure 2A for one such animal, the injection resulted in retrogradely labeled neurons in layer III of a sizeable area of MEC that in all experimental animals was part of the lesioned area (Figures 2B, 3A, and 3C). Some additional labeling of cells in layer II was caused by spreading of the dye into the dentate molecular layer (Figure 2A). A few labeled neurons were also observed in layer V. This may reflect uptake by weak projections from deep entorhinal layers to the hippocampus (Witter et al., 1989), but a more likely source is leakage of tracer into the white matter of the overlying cortex (Figure 2A), which contains axons from deep entorhinal neurons to cortical targets (Swanson and Köhler, 1986; Insausti et al., 1997). Isolated retrogradely labeled cells were only occasionally noted in any of the areas with damage outside the MEC (see below). Altogether, the staining pattern suggests that the tetrodes were placed in an area of CA1 that, in normal animals, received dense input from layer III neurons in the target area of the GAG infusion.

Lesions in Entorhinal Cortex

All seven animals in the lesion group with tetrode implants in CA1 had damage ipsilateral to the injection site in entorhinal cortex, as measured by a qualitative assessment of cell loss, comparing ipsilateral and contralateral hemispheres as well as lesioned and control animals. In all animals, the lesion included the center of the ipsilateral MEC, typically most of the intermediate MEC and some of the adjacent dorsocaudal MEC. The lesions in MEC were mostly confined to layer III with minor or no damage in layers II and V, as shown in Figures 2B and 3A (examples of layer II and layer V damage are indicated by arrowheads). The size of the lesion showed some variation, with patches of spared tissue in most animals (Figures 2B and 3), but the specificity to layer III was maintained in all cases. In three animals, the contralateral EC showed detectable cell loss, primarily in layer III. These animals, and one additional rat, also showed damage in layers II–V of ventral and lateral parts of the ipsilateral lateral entorhinal cortex (LEC). Small regions of cell loss were seen in layers II–VI of perirhinal cortex in two of these animals. Finally, in a limited number of sections from two animals, minor damage was seen in the anterior part of the ventral claustrum and in the overlying parts of the posterior piriform cortex.

Layer III lesions in MEC are observed only when the GAG infusion is followed by a short period of epileptic seizures (Wu and Schwarcz, 1998; see Experimental Procedures). It is possible that these seizures also induced diffuse cell degeneration outside the MEC to an extent that was too small to be detected with the cresyl violet and NeuN stains. Such degeneration might

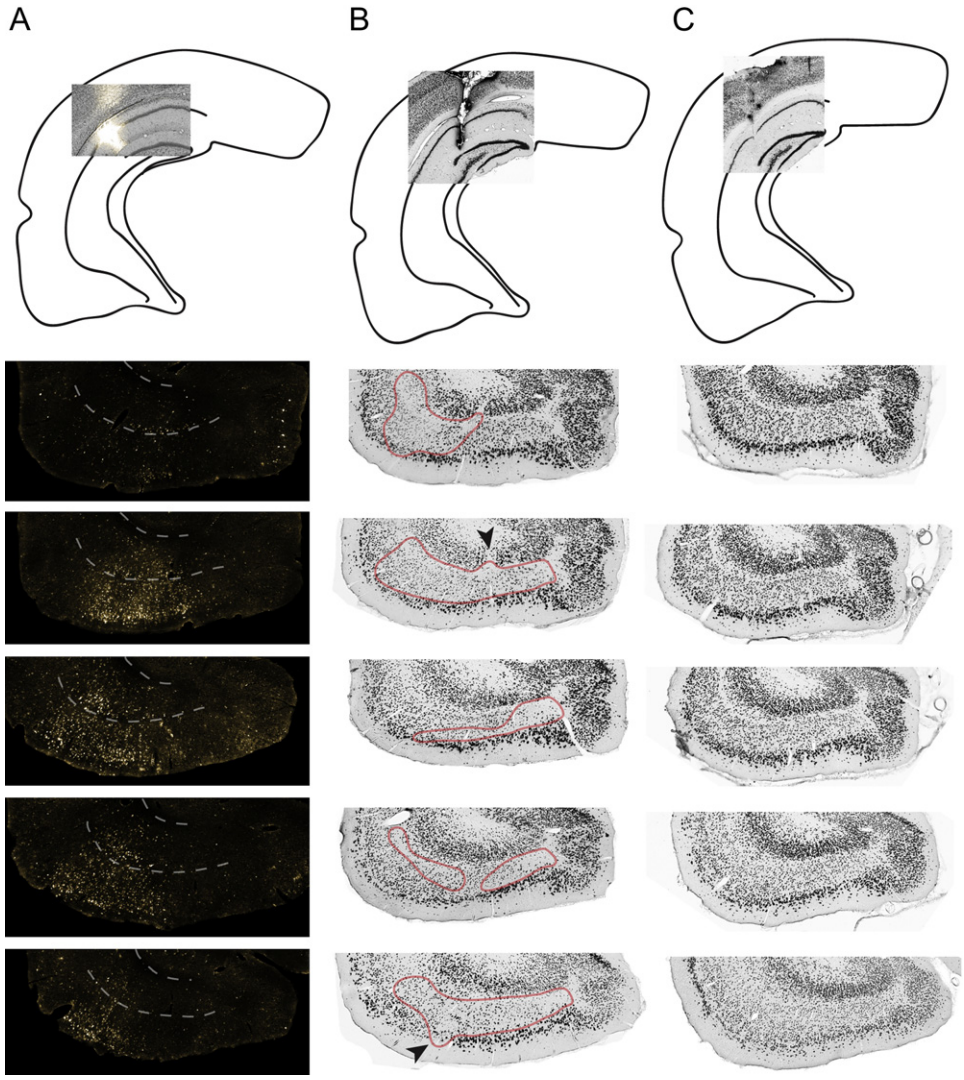

Figure 2. Connectivity between the Lesion Area in Layer III of Entorhinal Cortex and the Recoding Site in Hippocampal Area CA1

The upper row shows coronal NeuN-stained sections from the hippocampus; the five lower rows show horizontal sections at successively more ventral levels, all including the entorhinal cortex. Sections are spaced by approximately 0.5 mm.

(A) Injection of the retrograde tracer Fluorogold (light yellow color on the NeuN-stained section) at the coordinates used for hippocampal unit recording results in labeling in an area of MEC that overlaps with the lesioned zone (red outline in [B]). Gray stippled lines indicate the angular bundle and the lamina dissecans.

(B) Recording site in CA1 and lesion in the entorhinal cortex of a GAG-injected animal. The lesion (outlined in red) is largely restricted to layer III with some additional damage to layers II and V (arrowheads).

(C) Recording site in a control animal and horizontal sections of the intact entorhinal cortex. Note the difference in cell density in layer III between (B) and (C).

occur, for example, in the hippocampal inputs to CA1 or in areas providing inputs to layers II and III of the entorhinal cortex. To map the cell loss with a more sensitive approach, we first assessed neuronal degeneration in four lesioned animals not implanted for recording, making use of a specific marker for neuronal degeneration, Fluoro-Jade B (Schmued and Hopkins, 2000). One week after the GAG infusion, we observed a restricted lesion of layer III in the central part of MEC and no additional damage in any other part of the hippocampus or parahippocampus (Figure 3B). Almost no cells in layer III survived in the center of the lesion, suggesting that the output from layer III to the corresponding part of CA1 was strongly compromised in our preparation. Because some of our experimental animals showed minor damage outside of the area showing degeneration 1week after GAG injection, we next stained for Fluoro-Jade B in two animals 4 weeks after the initial GAG application, which corresponds to the typical delay from surgery to the recording of place cells. In these animals, we observed occasional labeling of degenerating cells in the ventral portion of the LEC, but no neuronal degeneration in the hippocampal fields (i.e., dentate gyrus including the hilus, CA1–3, and subiculum) or in the pre- and parasubiculum. There was no further damage in MEC. The late additional damage is similar to what has been described after shorter survival times with another neurotoxin, aminooxyacetic acid, in the

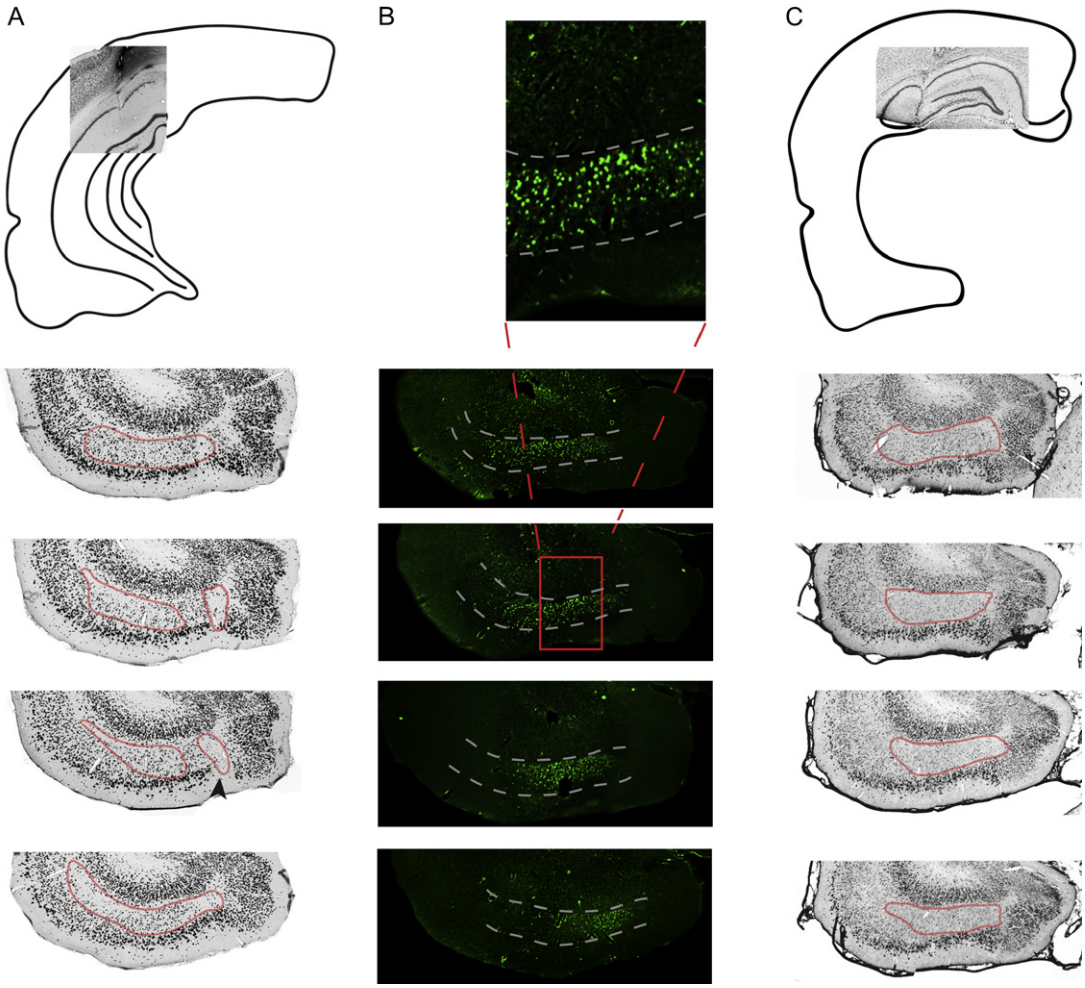

Figure 3. Labeling of Degenerating Neurons by Fluoro-Jade B Shows that the Lesion Is Selective for Layer III of the Entorhinal Cortex

(A) The recording site (upper picture, coronal section) and the lesioned area in layer III of the MEC (outlined in red on the horizontal sections) shown at four dorsoventral levels in an animal from which cells were recorded in CA1.

(B) Fluoro-Jade B labeling of damaged neurons in the MEC 1 week after injection of the neurotoxin GAG. The distribution of label is shown at increased magnification (top) for one of the sections. Note that labeling is restricted to layer III. Note also the correspondence between the area of labeled cells in (B) and the outline of the lesion in (A) and in Figure 2B. The dorsoventral levels of the horizontal sections in (B) correspond to those in (A).

(C) Example of recording site and lesion in one of the animals with recordings from CA3.

entorhinal cortex (Du et al., 1998). Note that Fluoro-Jade labeling is strongest around 1 week after the cells die (Eisch et al., 1998; Schmued et al., 1997), such that the initial neuronal degeneration in MEC was not detectable by 4 weeks. The consistent absence of damage in the hippocampal formation is in agreement with the findings by Wu and Schwarcz (1998), who reported that hilar cell loss was prevented by a combined application of GAG and the NMDA receptor antagonist MK-801, which prevented behavioral convulsions similar to what was achieved in this study with the application of the benzodiazepine clonazepam.

To further explore the structural impact of the GAG lesion in the hippocampus, we stained three lesioned brains with antibodies against vimentin, a marker for activated glia (Dahl et al., 1981; Khurgel et al., 1995). Using a protocol that preferentially stains glial processes, we observed labeling predominantly in stratum lacunosum-moleculare of CA1, the terminal zone of the lesioned direct entorhinal input (Figure 4A). The staining in CA1 was bilateral but more widespread on the lesioned than the nonlesioned side. Additional immunoreactivity was present in the hilar domain directly below the dentate granule cell layer, where glial extensions radiated in between granule cell bodies, and in the alveus, the angular bundle and the cortical white matter. Minor staining was noticeable in stratum radiatum of CA1. In the entorhinal cortex, some staining coincided with the cannula tract, but no staining was seen otherwise in layers II and V (Figure 4A). The specificity of the lesion implied by the vimentin stains was reinforced by analyses of Golgi-impregnated material, which showed that the entire dendritic tree, including the distal perforant-path terminal area, was preserved in GAG infused animals (Figure 4B). Taken together, these findings suggest that the structural lesion was largely confined to layer III of entorhinal cortex, with some synaptic reorganization in the

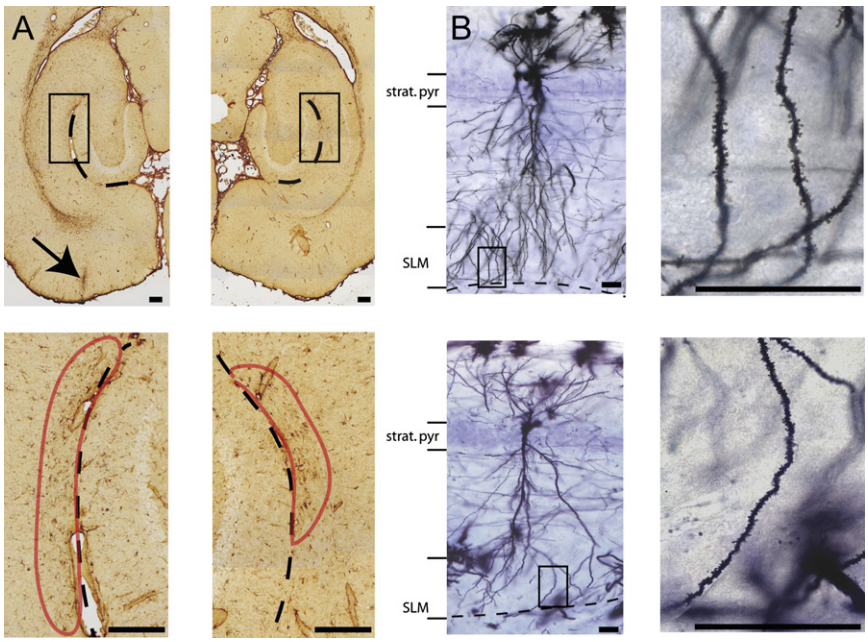

Figure 4. Activated Glia (A) and Neuronal Morphology (B) Indicate that Changes in GAG-Lesioned Animals Are Mainly Confined to Layer III of MEC and the Associated Terminal Zone of in CA1

(A) Immunostain against vimentin in a rat with a unilateral GAG lesion (arrow in left upper panel). Labeled glial processes are predominantly present bilaterally in stratum lacunosum-moleculare of CA1, the terminal zone of the lesioned direct entorhinal input. Notice that staining on the lesioned site is more widespread than on the nonlesioned side (lower left and right panels, respectively). Additional immunoreactivity is seen in the hilar domain directly below the dentate granule cell layer, extending in between granule cell bodies, and in the alveus, the angular bundle and the cortical white matter. In the entorhinal cortex, some staining is seen around the cannula tract (arrow in upper left hand panel). Scale bars equal 250 μm.

(B) Horizontal sections showing Golgi-impregnated CA1 neurons in a control animal (upper panel) and a GAG-lesioned animal (lower panel). Sections were taken at corresponding hippocampal positions. The entire dendritic tree, including the distal part that receives perforant-path terminals, appears quite intact in both cases. High-power images of the distal dendrites (upper and lower most right hand panels) illustrate that in the lesioned animal dendrites may show lower spine densities locally, in addition to occasional elongation of spines and some reduction in diameter of the most distal tips. However, no major differences in spine densities and dendritic diameters were apparent. Scale bars equal 50 μm.

denervated zone in CA1 and associated portions of stratum radiatum, but with little, if any, neuronal degeneration in the hippocampus itself.

Place Cells in CA1

The dentate-CA3 network has a rich associational capacity (Amaral and Witter, 1989) that might serve as a neuronal architecture for storage of information in the hippocampus (Marr, 1971; McNaughton and Morris, 1987; Nakazawa et al., 2002; Steffenach et al., 2002). The storage of spatial information in CA3 is not instantaneous, as the ensemble of active place cells in CA3 undergoes considerable change during the first 10–20 min of exposure to a novel environment (Leutgeb et al., 2004, 2006). Deletion of NMDA receptors in CA3 slows down the development of stable place fields in CA1 (Nakazawa et al., 2003), suggesting that the maturation of representations in CA3 may be followed by equally slow or even slower changes in CA1. Thus, to maximize the possibility of detecting influences of CA3 inputs on place-cell activity in CA1, we first recorded activity during running in a familiar box in a familiar room after 1 to 2 weeks of daily training in the environment. At this stage of training, we assumed that representations in CA1 had generally reached a stable state reflecting inputs from both CA3 and entorhinal cortex (Lever et al., 2002).

Pyramidal cells in CA1 of animals with intact entorhinal cortices were mostly sharp and focused (Figure 5). Most cells had a single firing field covering 20%–25% of the box surface, comparable to, or marginally larger than, the field size of place cells recorded at more septal locations in the CA1 in the same behavioral task in previous studies (Leutgeb et al., 2004). In contrast, place fields recorded from animals with entorhinal layer III lesions were generally wider and more dispersed (Figure 5). The size of the primary field was larger than in the control animals (0.358 ± 0.044 m^2 versus 0.254 ± 0.036 m^2; median ± SE of the median; Mann-Whitney test $Z = 2.22$, $p < 0.05$), and the firing fields were less coherent (0.72 ± 0.04 versus 0.83 ± 0.08; $Z = 2.07$, $p < 0.05$). The lesions strongly reduced the information density of the place fields (lesions, 0.47 ± 0.08; controls, 0.71 ± 0.08; $Z = 2.81$, $p < 0.005$), and their sparsity was increased (lesions, 0.56 ± 0.04; controls, 0.45 ± 0.03; $Z = 2.92$, $p < 0.005$). The lesion did not cause significant changes in average rate (lesions, 1.20 ± 0.27; controls, 1.34 ± 0.23; $Z = 0.12$), peak rate (lesions, 8.66 ± 0.93; controls, 11.32 ± 1.08; $Z = 1.69$), or percentage burst activity (lesions, 20.37 ± 3.55; controls, 23.66 ± 1.92; $Z = 0.28$), which speaks against a nonspecific change in the basic physiological properties (e.g., resting membrane potential) of the CA1 cells.

The distribution of the spatial information density scores showed a clustering of cells from lesioned animals at the lower end of the scale (Figure 5). When the cells from both groups were ranked by their information density, 19 of the 20 cells with the lowest score (i.e., the weakest spatial modulation) came from rats in the lesion group. Among the 20 cells with the highest information density, 9 came from lesioned rats. The total number of cells from each experimental group was similar (lesions, 49 cells; controls, 44 cells). Cells with different degrees of spatial modulation were typically seen in the same lesioned animal (see Figure 5A for a representative example; black horizontal lines indicate cells from the same animal). This suggests that the lesion did not result in a general network dysfunction but affected subsets of CA1 cells rather selectively.

To substantiate the observed impact of entorhinal layer III lesions on place fields in CA1, we recorded from the same cells

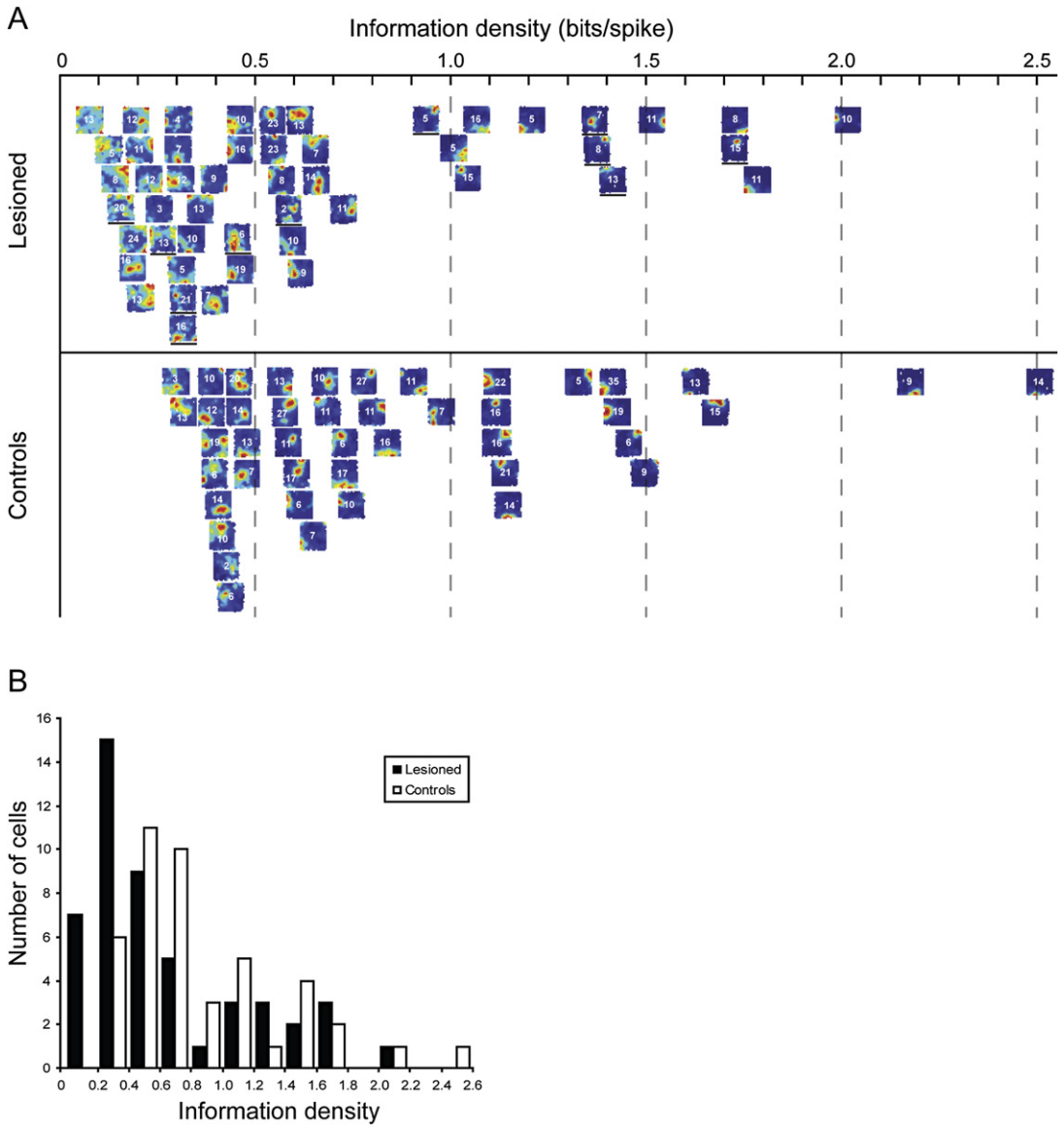

Figure 5. Place Representation in the Hippocampal CA1 Area Is Impaired after Removal of Direct Input from Layer III in Entorhinal Cortex

(A) Rate maps for all CA1 cells from lesioned and control animals recorded in the familiar environment (one map per cell). The rate maps are positioned along the x axis according to their information density. White pixels indicate areas not visited by the rat; dark red corresponds to the maximum firing rate and dark blue to no firing. Numbers on the rate maps indicate the peak firing rate (in Hz). Black horizontal lines below the rate maps mark a set of cells recorded in the same lesioned animal.

(B) Distribution of information density scores for the entire sample of CA1 place fields recorded in the familiar environment in the lesion and control groups. Note that the distribution is shifted toward zero in the animals with layer III lesions in MEC.

in a second environment, a novel enclosure in a novel room. Recordings began immediately as the rat entered the novel apparatus and lasted for 30 min. In both experimental groups, CA1 pyramidal cells showed weaker spatial modulation in the novel environment than in the familiar environment (Figure 6), as expected (Leutgeb et al., 2004; Wilson and McNaughton, 1993), but as in the familiar environment, the firing was more dispersed in the lesioned animals than the control animals. Place cells from lesioned animals had less coherent fields ($Z = 2.34$, $p < 0.01$) and the information density scores were lower, fluctuating around 0.2 ($Z = 2.25$, $p < 0.05$; see Figure 5 for examples of information density values). The average place field size was not significantly different between the groups ($Z = 1.19$, n.s.), but this may reflect a ceiling effect as the fields covered more than half of the environment. The increase in place field size compared to the familiar environment was significant in both groups (Wilcoxon signed ranks test, lesions, $Z = 2.55$, $p < 0.01$; controls, $Z = 2.40$, $p < 0.01$), as was the loss of spatial coherence (lesions, $Z = 4.26$, $p < 0.001$; controls, $Z = 2.44$, $p < 0.01$), and the reduction in information density (lesions, $Z = 4.82$, $p < 0.001$; controls, $Z = 3.86$,

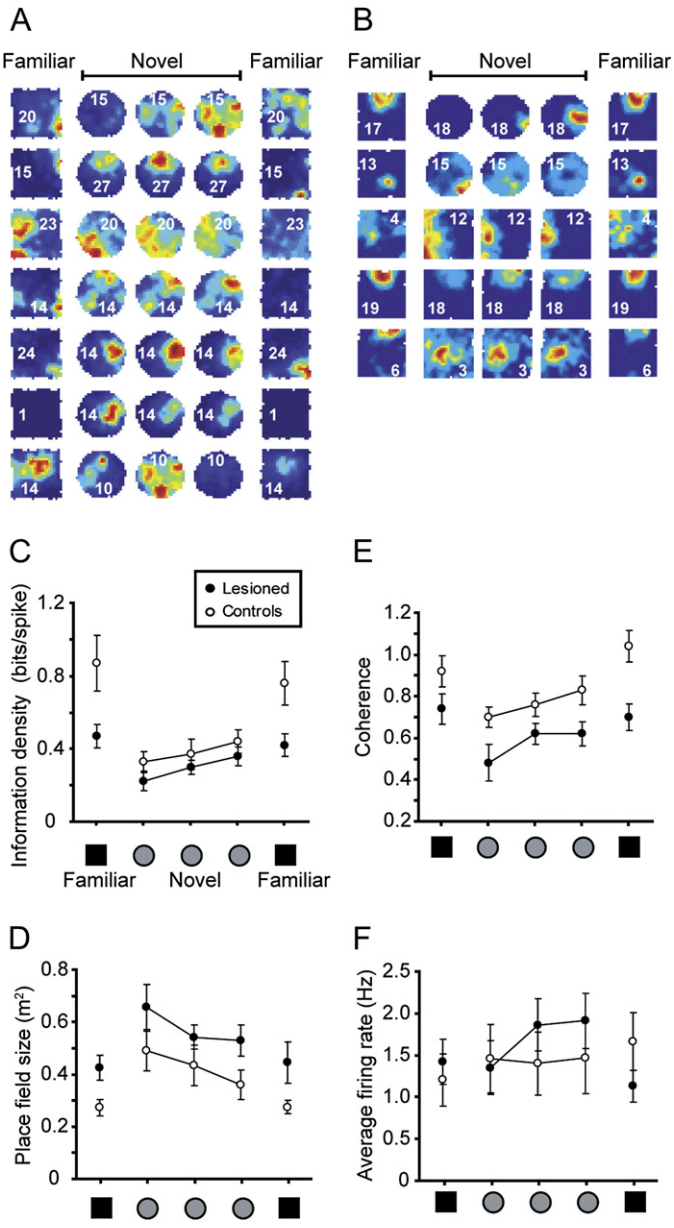

Figure 6. Disruption of Localized Firing in a Novel Environment

(A and B) Place fields of simultaneously recorded CA1 cells in a familiar and a novel environment in a layer III-lesioned animal (A) and a control animal (B). Symbols as in Figure 5.

(C–F) Group medians of (C) information density, (D) place field size, (E) spatial coherence, and (F) average firing rate are plotted for the familiar and novel environment. Error bars indicate the standard error of the median.

$p < 0.001$). Both groups developed more localized place fields across blocks of 10 min in the novel environment (Figures 6C and 6D; Friedman nonparametric ANOVA for information-density scores, lesions, $F(2) = 18.0$, $p < 0.001$; controls, $F(2) = 11.9$, $p < 0.005$), although the place fields did not become as sharp as in the familiar environment. Taken together, the observations in the novel environment confirm the impairment observed in CA1 of the lesioned animals in the familiar environment.

To establish if stability of firing can be maintained in CA1 place cells without direct entorhinal input, we finally compared CA1 fields in lesioned animals on two separate trials in the same familiar environment. The interval between the trials was 1 hr. Rate maps for the two recordings were highly correlated in both experimental groups, with a minor but significant reduction in the GAG group (lesions, 0.79 ± 0.03; controls, 0.86 ± 0.02; $Z = 2.51$, $p < 0.05$). A similar difference was observed when the trials in the familiar room were separated by an intervening trial in a novel room (lesions, 0.70 ± 0.07; controls, 0.88 ± 0.02; $Z = 3.32$, $p < 0.001$). These small differences may be a consequence of increased variability in firing location in the GAG animals. This interpretation is supported by significant correlations between stability (spatial correlation) and information density in both groups on both tests (lesions, $r \geq 0.56$, $p < 0.001$; controls, $r \geq 0.48$, $p < 0.05$).

Place Cells in CA3

The impairment in spatial firing in CA1 may be caused by disruption of direct perforant-path input from layer III of entorhinal cortex, or the entire hippocampal network may be compromised, as predicted, for example, if the impairment reflected epileptic seizures. To distinguish between these possibilities, we recorded place fields from the CA3 area of the hippocampus in a new set of four rats with layer III lesions and five controls (Figure 7). Because entorhinal inputs to CA3 cells originate in layer II, which should be largely preserved by the GAG lesion, we expected impairments in place fields in this area only if the lesions led to a general disruption of hippocampal functions.

The tetrodes were aimed for a part of the proximal CA3 that projects strongly to the part of CA1 where place cells were recorded in the main part of the study (Figure 3C, top panel). The electrodes were placed in the intermediate-to-proximal part of CA3, which provides most of the output to the proximal-to-intermediate recording location in CA1. They were placed anterior and medial to the CA1 electrodes, at a position where the widely distributed axonal projections of the CA3 cells overlap significantly with the CA1 recording area (Figure 7D). This position was selected to facilitate recording in an area of CA3 connected to both the CA1 recording area as well as the lesioned area in layer III of MEC. Lesions in the four animals with CA3 tetrode implants were as specific to layer III neurons as in the CA1 study and the spatial extent of the lesion in the two parts of the study was comparable (Figure 3C, bottom panels). The lesions included the center of the ipsilateral MEC, most of the intermediate MEC and some of the adjacent dorsocaudal MEC. The lesions in MEC were mostly confined to layer III with minor or no damage in adjacent layers.

There was no detectable impairment in spatial representation in CA3 following lesions in layer III of entorhinal cortex. The firing fields were sharp and confined and not different from those of the control group (Figure 7A and C). There was no difference in information density (lesions, 1.02 ± 0.11; controls, 0.82 ± 0.16; $Z = 0.85$, n.s.), size of the place field (lesions, 0.248 ± 0.038 m^2;

controls, 0.300 ± 0.064 m^2; Z = 0.69, n.s.), sparsity (lesions, 0.35 ± 0.03; controls, 0.40 ± 0.05; Z = 0.38, n.s.), or spatial coherence (lesions, 0.92 ± 0.08; controls, 0.87 ± 0.11; Z = 0.36, n.s.). There was no significant change in average rate, peak rate or burst activity. In one lesioned animal, the electrodes penetrated CA1 and the dentate gyrus on their way down to CA3 and recordings were made in all three areas on separate days (Figure 7B). CA1 cells showed a striking deficit in spatial modulation, as in the main experiment (Figures 5 and 6), whereas neurons in CA3 and dentate gyrus showed no striking change. Although the number of cells in each area of this animal was too low for statistical analysis, the pattern of results and the absence of impoverished spatial representation in CA3 points to the direct perforant-path input as the likely source of the reduced spatial specificity of CA1 cells after GAG lesions in entorhinal cortex.

DISCUSSION

We have shown that the localized firing pattern of place cells in hippocampal area CA1 is significantly attenuated by selective ipsilateral lesions in entorhinal layer III, which provides most of the direct cortical input to the CA1 field. Place fields increased in size, and their spatial coherence and information density were reduced. Layer III lesions were not accompanied by detectable impairments in the CA3 place representation. The results indicate that the direct pathway from entorhinal cortex to CA1 is necessary for accurate location-specific firing in the CA1 pyramidal-cell population.

Significance of the Direct Pathway

The significance of the direct pathway for normal operation of the CA1 circuit is consistent with the relative maintenance of both place-specific firing and hippocampus-dependent spatial recognition memory in animals with complete lesions of CA3 (Brun et al., 2002). Following such lesions, cortical input is available to CA1 only by direct connections, suggesting that the remaining CA1-subiculum-entorhinal circuit may perform at least some neuronal computations without additional input from the dentate gyrus and CA3. The present study extends these findings by showing that direct perforant-path input from layer III is necessary for normal spatial firing in the place cell population of CA1. The contribution of the direct pathway is probably underestimated by the present results because of possible sprouting or potentiation among the remaining inputs to the pyramidal cells in CA1 during the postoperative recovery period (Gloveli et al., 2003; Shah et al., 2004; Shao and Dudek, 2004; Siddiqui and Joseph, 2005). The implication of a necessary role for the direct pathway is consistent with the impairment in long-term memory consolidation in animals where the direct pathway from the entorhinal cortex to CA1 is transected after spatial learning (Remondes and Schuman, 2004), although this impairment could, in principle, reflect damage to the outputs as well as the inputs of the hippocampus. The apparent significance of the direct entorhinal pathway is at odds, it seems, with the poor induction of somatic action potentials in CA1 pyramidal cells after single-pulse stimulation of the perforant path in hippocampal slices (Jarsky et al., 2005). Distal dendritic signals propagate more reliably during burst stimulation, however, suggesting that a minimal level of temporal summation may be required (Jarsky et al., 2005). Spatial summation between converging entorhinal inputs may have a similar facilitating effect on the propagation of dendritic signals, but the contribution of spatial summation may be more difficult to detect in the hippocampal slice preparation, where a significant fraction of the entorhinal axonal input is lost. The significance of intact entorhinal fibers is supported by the more reliable induction of action potentials in CA1 after stimulation of the perforant path in vivo and by the fact that such discharge is detectable only when stimulation and recording electrodes are placed in register within a narrow spatial window of the perforant path (Naber et al., 1999).

A key question is why some place cells lost their spatial tuning after cell loss in layer III while others remained as localized as in the controls. One possibility is that the sharpest CA1 place fields were maintained by CA3 neurons, whose spatial modulation was not affected by the lesion; another is that cells with strongly defined fields received a larger input from surviving neurons in layer III of the MEC. Considering that the collaterals of an entorhinal layer III axon cover a significant portion of the longitudinal CA1 axis (Naber et al., 2001), it is quite likely that some CA1 cells in the lesion group were contacted by axons from the spared regions of layer III. Some inputs may also come from layer III neurons in the contralateral entorhinal cortex, although the commissural projection at the level we recorded from is rather weak (Steward, 1976). The latter possibility is reinforced by the fact that, in contrast to the diffuse and widespread projections of the Schaffer collaterals (Li et al., 1994), the projection from layer III to CA1 has more targeted functional effects (Buzsaki et al., 1995; Naber et al., 2001), implying that the organization of the presynaptic entorhinal input could be more point-to-point-like. If this is the case, some CA1 cells could have lost most if not all of their direct ipsilateral input from MEC after a partial layer III lesion, while their nearest neighbors might still receive virtually intact input from surviving neurons. The result would be a heterogeneous response in CA1, even at a single recording location. Although the present data do not rule out an additional role for CA3 inputs in shaping place fields in CA1, the lack of impairment in the CA3 place cells clearly shows that direct entorhinal input is necessary for sharp and confined place representations in the CA1 cell population as a whole. A more complete understanding of how inputs from CA3 shape place fields in CA1 must await the future availability of specific tools for separate and total inactivation of the two afferent cell populations.

Significance of the Indirect Pathway

The necessary role of the direct pathway in place-specific activity does not preclude a critical involvement of the indirect pathway in hippocampal network functions more generally. The slow development of new firing fields, as observed in the unfamiliar environment, raises the possibility that the contribution of Schaffer-collateral input to localized firing in CA1 evolves with experience in the environment. As reported previously for the dorsal hippocampus (Frank et al., 2004; Leutgeb et al., 2004; Wilson and McNaughton, 1993), place fields in CA1 were broader and more irregular in a novel environment than in an environment where the animal had been trained for several weeks. This effect added to the impairment of the lesion group, where the fields covered more than

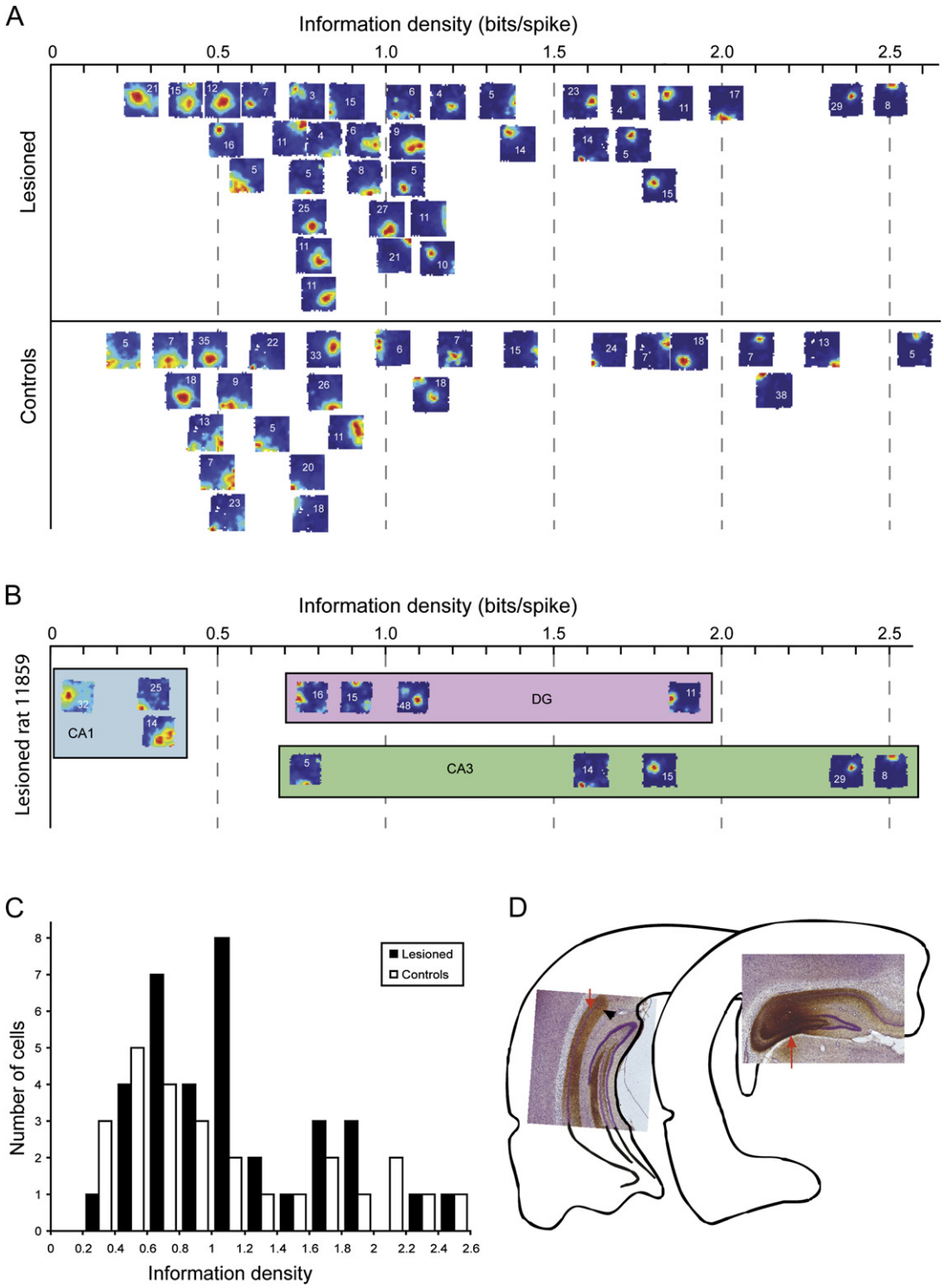

Figure 7. Place Representation in CA3 Is Not Affected Detectably by an Entorhinal Cortex Layer III Lesion

(A) Rate maps for all CA3 cells from lesioned and control animals recorded in a familiar environment, plotted as in Figure 5.

(B) Firing fields from CA1, CA3, and dentate gyrus (DG) in a single lesioned rat recorded on 3 different days. Only CA1 fields appear to be impaired.

(C) Distribution of information density scores for the entire sample of CA3 place fields recorded in the familiar environment in the lesion and control groups. The distributions are not different.

(D) Light micrographs showing axonal projection pattern of a group of labeled pyramidal cells in the part of CA3 where place cells were recorded after layer III lesions in entorhinal cortex (red arrow in right panel). The black arrow in the left panel indicates the border between CA1 and subiculum. Note the extensive and

half of the box in the novel environment. The direct inputs from the entorhinal grid-cell network are therefore critical at a stage where hippocampal firing may rely more on preconfigured path integration-based representations than on established associations with specific landmarks stored, for example, within the hippocampus.

After prolonged training, place fields in CA1 became more specific in both groups, as seen in the familiar environment. In CA3, the formation of stable representations during exploration of an open field is known to require multiple epochs of experience under some conditions (Leutgeb et al., 2004, 2005a, 2006). The increase in spatial selectivity in CA1 in the lesion group suggests that, over the course of several days, spatial information may eventually be conveyed to this subfield from CA3. The experiments in the familiar environment suggest, however, that location-selective inputs via the indirect pathway cannot, by themselves, support localized firing at the same level of precision as in intact animals, not even after prolonged training.

What is then the function of sequential transmission through the trisynaptic circuit? Converging evidence suggests that dynamic representations of place are computed in the entorhinal cortex and associated cortical areas (Fyhn et al., 2004, 2007; Hafting et al., 2005; Hargreaves et al., 2005; Sargolini et al., 2006) and that the hippocampus instead integrates the output from the spatial map in the entorhinal cortex with nonspatial and contextual information specific to each individual environment (Leutgeb et al., 2005b, 2005c). Incoming spatial information from layer II of the entorhinal cortex is orthogonalized into distinct nonoverlapping representations as signals enter the dentate gyrus and CA3 (Leutgeb et al., 2004, 2007; Fyhn et al., 2007), and cell ensembles in CA3 have significant capacity for retrieving these representations from degraded versions of the input during subsequent recall (Lee et al., 2004; Nakazawa et al., 2002). Output from the associative network in CA3 may in turn control the formation of representations in CA1 in close temporal interaction with specific spatial information conveyed from entorhinal grid cells through the direct pathway (Dragoi and Buzsaki, 2006; Hasselmo et al., 2002; Jarsky et al., 2005; Remondes and Schuman, 2002).

EXPERIMENTAL PROCEDURES

Subjects

A total of 42 male Sprague-Dawley rats (2–3 months old, 300–400 g) were used. Twenty-nine of the animals were used for electrophysiological recordings, three for Fluorogold tracing experiments, four for Fluoro-Jade B labeling experiments, three for Golgi staining, and three for Vimentin labeling experiments. All rats were maintained on a 12 hr light/12 hr dark schedule, and all testing occurred in the dark phase. The animals used for electrophysiology were housed individually and kept at 85%–90% of their initial weight to motivate food searching. Water was available ad libitum.

Surgery

The rats were anesthetized with Equithesin (1 ml/250 g; i.p.). Thirteen control animals and seven lesioned animals were implanted with tetrodes aimed for CA1, while five control animals and four lesioned animals received tetrodes aimed for CA3. Four tetrodes of twisted 17 μm HM-L coated platinum-iridium wire were connected to a microdrive to allow dorsoventral adjustment of the tetrodes after surgery (Hollup et al., 2001). In most cases, the tetrodes were fortified by one-component epoxy which cured after 30 min at 200°C. The electrode tips were platinum-plated before surgery in order to reduce electrode impedances to 150–250 kΩ at 1 kHz. The tetrodes were positioned above the hippocampus at an intermediate septotemporal level (AP 5.7, ML 4.7, DV 1.4 for CA1 recordings; AP 5.1, ML 4.1, DV 1.7 for CA3 recordings). Animals in the lesion group received a unilateral 1.12 μl injection of γ-acetylenic GABA (GAG, 4.0 mg/ml) through a 28 gauge cannula (C313I; Plastics One). The injection was placed into the MEC with the cannula angled 18 degrees in the anterior direction and entering the brain just anterior of the transverse sinus. The injection volume was delivered unilaterally at three different dorsoventral levels (ML 5.0, DV 4.0, 3.5, and 3.0). A mechanical pump (CMA Microdialysis) ensured a stable infusion speed of 0.1 μl/min. Control animals received no injection or cannula in the entorhinal cortex. The microdrive was secured to the scull using jeweler's screws and dental cement. A jeweler's screw fixed to the skull served as a ground electrode. As soon as the GAG-infused rats woke up from anesthesia they exhibited behavior consistent with epileptic seizures (wet-dog shakes, decreased responsiveness, short periods of "frozen posture," and in some cases occasional forelimb clonus). A brief period of postsurgical epileptic seizures is necessary for cell loss in layer III after GAG infusion (Wu and Schwarcz, 1998). Five to seven hours after the injection, the rats received an injection of clonazepam (0.35 mg/kg) i.p to block further seizures.

Unit Recording and Tracking

Daily screening for cells and behavioral training started 2–3 days after surgery. The tetrodes were lowered over several days in steps of 50 μm until hippocampal units could be identified. The rats were connected to the recording equipment via AC-coupled unity-gain operational amplifiers (Axona Ltd.), with counterbalanced hearing-aid wire allowing the animal to move freely within the enclosure (Hollup et al., 2001). Recorded signals were amplified 15,000 to 25,000 times and band-pass filtered between 0.8 and 6.7 kHz. Triggered spikes were stored to disk at 48 kHz (50 samples per waveform, 8 bits/sample) with a 32 bit time stamp (clock rate at 96 kHz). EEG signals from the hippocampus were amplified 3000–5000 times, lowpass-filtered at 125 Hz, and stored at 250 Hz (8 bits/sample). A tracker system (Axona Ltd.) was used to record the position of a red LED attached to the head stage at a rate of 50 samples per second. The tracked position was smoothed offline with a 15 point median filter.

Familiar Environment

Hippocampal activity was recorded while rats were running in a black aluminum enclosure (100 × 100 × 50 cm high) resting on a table in the center of a room with multiple background cues (curtains were not used). The floor was covered by a dark rubber mat and a white cue card (50 × 50 cm) was centered on one of the box walls. Each recording lasted for 10 min. Crumbs of chocolate cereal were scattered individually into the box at 30–60 s intervals to motivate continuous running. Recordings began when the rat covered the whole box surface and ran continuously, usually after about 7 days of training. The rats were never exposed to the recording rooms before surgery. The floor of the recording apparatus was washed with water before each recording. Immediately before and immediately after each experiment, spikes were recorded for 5 min while the rat rested in a flower pot on a pedestal outside the recording apparatus. When the recording in the flower pot was completed, the rats were returned to their home cages in the animal quarter. For animals with CA1 units, a second recording in the familiar environment was made 1–2 hr after the first recording.

Novel Environment

After the second test in the familiar environment, the rat was transported to a novel room with a novel box for exploration. The surface of the box was

widespread axonal projection pattern throughout CA1. The estimated average recording location in CA1 (red arrow in left panel) was clearly within the terminal field of the axon of the CA3 cell.

normally a circle, but on four trials in lesioned animals and five trials in controls, a square was used. The circular box was 95 cm in diameter and either black, gray or steel-colored with one prominent cue card (20 cm wide, 30 cm high) of a contrasting color on the wall. The square box was either a 105 × 105 cm white box or an 80 × 80 cm gray box; the walls of all enclosures were 50 cm high. The cue card was fixed midway between two corners in these boxes. Recordings began immediately after the rat was placed in the box, approximately 1–2 min after it was brought into the room. After 30 min of recording, the rat returned to the familiar environment for another 10 min recording.

Cell Separation

Spike sorting was performed off-line using graphical cluster-cutting software (Axona Ltd.). Pyramidal cells and interneurons were distinguished by the width of the extracellular action potential, firing pattern (i.e., complex spikes) and average firing rate (Hollup et al., 2001). To estimate the quality of the cluster separation, we calculated the isolation distance for each putative cell (Harris et al., 2001; Schmitzer-Torbert et al., 2005). Isolation distance is the radius of the smallest ellipsoid from the cluster center containing all its spikes and an equal number of spikes from other clusters. The measure is scale invariant and estimates the distance from the current cluster to the nearest other cluster. Thus, a cluster far away from other recorded spikes in the multidimensional cluster cutting space gets a high value.

Place Field Analysis

A total of 154 cell clusters were accepted for further analysis (49 clusters from 7 lesioned rats with CA1 recordings, 44 clusters from 13 CA1 control rats, 35 clusters from 5 CA3 recordings in lesioned rats, and 26 clusters from 4 CA3 controls). To characterize their place fields, a spike density function was estimated by convoluting the spike train (sum of Dirac delta functions) with a Gaussian smoothing kernel. The spike density function was sampled synchronously with the position tracker, and a rate map was calculated for pixels of 5 × 5 cm visited by the rat. Only cells that had average firing rates above 0.25 Hz in one environment were included in the analysis for that environment. A "place field" was defined as a contiguous region of at least 8 pixels (200 cm^2) where the firing rate exceeded 20% of the peak rate (Muller et al., 1987). "Place field size" was defined as the size of the largest detected field (Muller et al., 1987). The "information density" (Skaggs et al., 1993) estimates how much information a single spike conveys and is defined by the formula

$$I = \sum_{i=1}^{N} p_i \frac{\lambda_i}{\lambda} \log_2 \frac{\lambda_i}{\lambda}$$

where I is the information density measured in bits per spike, i is the index of the pixels of the place field, p_i is the probability of the rat being at location i, λ_i is the average firing rate of the cell when the rat is at location i, and λ is the total average firing rate. The sparsity of the rate map (S) was similarly calculated by dividing the square mean rate by the mean square rate over all pixels (Treves and Rolls, 1991; Skaggs et al., 1993):

$$S = \frac{\lambda^2}{\sum_{i}^{N} p_i (\lambda_i)^2}.$$

Spatial "coherence" was estimated as the first order spatial autocorrelation of the place field map and measures the extent to which the firing rate in a pixel is predicted by the rates of the neighboring pixels (Muller and Kubie, 1989). The coherence was calculated without smoothing the fields. The stability of firing fields across repeated trials in the same box was estimated with a spatial correlation procedure where the rates of firing in corresponding pixels of the two maps were correlated pixel-wise for each cell. Bins visited less than 150 ms in either room were excluded to avoid artifacts in the correlation measure.

Histology

At the end of the experiment, the rats received an overdose of Equithesin and were perfused transcardially with saline and 4% formaldehyde. The brains were stored in 4% formaldehyde before they were frozen and cut into 30 μm slices on a cryostat or microtome. Initially, brains were cut in the sagittal plane to assess both the position of the recording tetrode and the position and extent of the lesion in the same orientation. These brains were stained with cresyl violet. However, the extent of the lesion could not be easily assessed in sagittal sections, so in the remaining animals, most of the entorhinal cortex, including the intended lesion site, was cut horizontally, whereas the dorsal part of the brain was cut coronally to assess the tetrode position in the hippocampus. In order to visualize neuronal loss more clearly, these brains were stained with a marker for neuronal nuclei, NeuN (Mullen et al., 1992), and mounted on glass. Sections with fluorescent agents were studied with a Zeiss or Leica fluorescence microscope with a mounted camera. All pictures of the histology were processed in Adobe Photoshop and Adobe Illustrator for assembling the figures.

Anterograde and Retrograde Tracing

To verify whether the recording area in CA3 provides input to the recording area in CA1, we injected the anterogradely transported tracer Phaseolus vulgaris leucoagglutinin (PHA-L) in CA3. Injections were made with the use of a glass capillary through iontophoresis, using alternating current (7 s on/7 s of; 7 mA). Animals survived for 7–14 days and were transcardially perfused. Coronal sections were cut on a freezing sliding microtome, and sections were stained for PHA-L using the DAB method (see Wouterlood and Groenewegen, 1991). The data presented are from one animal, taken from a larger collection of tracer injections in CA3 of Wistar rats. The recording area in CA1 was identified by infusing the retrograde tracer hydroxystilbamidine (Fluorogold; Molecular Probes; 2.5% in 0.9% NaCl) with a syringe pump into the CA1 of three naive rats at the same coordinates as used for unit recording. The solution (0.1 μl) was infused over a 5 min period through a 33 gauge cannula (C315I; Plastics One). The cannula was retracted 10 min later. The rats survived for 6 days and were subsequently perfused transcardially. The brains were extracted and stored in 4% formaldehyde before they were cut horizontally and coronally similar to the procedure for animals used for electrophysiological recordings.

Fluoro-Jade B Labeling of Degenerating Neurons

Four rats received GAG injections as described above and were perfused either 1 (n = 2) or 4 weeks (n = 2) after surgery. The brains were cut horizontally and stained with a neuronal marker for cell loss (Fluoro-Jade B; Schmued et al., 1997).

Vimentin Labeling

Three lesioned animals were perfused as above 1 week after the lesion. Two brains were cut horizontally at 30 μm as described above. The remaining brain was embedded in paraffin and 10 μm horizontal sections were mounted. All sections were stained with an antibody against vimentin (DakoCytomation) using 1:200 and 1:400 dilutions and avidin-biotin peroxidase methods (Vector labs, Netherlands).

Golgi Staining

Two lesioned animals and one unoperated control animal were perfused as above 1 week after the lesion. Blocks of brain tissue from all three animals were processed in parallel, using the FD Rapid GolgiStain kit according to the specifications of the supplier (FD Neurotechnologies, Inc). Horizontal sections of 100 μm thickness were counterstained with cresyl violet.

Supplemental Data

The Supplemental Data for this article can be found online at http://www.neuron.org/cgi/content/full/57/2/290/DC1/.

ACKNOWLEDGMENTS

We wish to thank K. Haugen, A.M. Amundsgård, R. Skjerpeng, I.M.F. Hammer, K. Jenssen, H. Waade, E. Sjulstad, and A. Ingrassia for technical assistance. Dr. W.S. van der Hel and S.A.M.W. Verlinde, Rudolf Magnus Institute of Neuroscience, Dept. of Pharmacology and Anatomy Univ. Medical Center, Utrecht, are acknowledged for advice and help with vimentin staining. The work was supported by the 5th Framework RTD Programme of the European

Commission, the Fondation Bettencourt-Schueller, NIH grant NS16102, and the Centre of Excellence scheme of the Norwegian Research Council.

Received: May 30, 2006
Revised: August 9, 2007
Accepted: November 21, 2007
Published: January 23, 2008

REFERENCES

Amaral, D.G., and Witter, M.P. (1989). The three-dimensional organization of the hippocampal formation: a review of anatomical data. Neuroscience *31*, 571–591.

Barnes, C.A., McNaughton, B.L., Mizumori, S.J., Leonard, B.W., and Lin, L.H. (1990). Comparison of spatial and temporal characteristics of neuronal activity in sequential stages of hippocampal processing. Prog. Brain Res. *83*, 287–300.

Brun, V.H., Otnass, M.K., Molden, S., Steffenach, H.A., Witter, M.P., Moser, M.B., and Moser, E.I. (2002). Place cells and place recognition maintained by direct entorhinal-hippocampal circuitry. Science *296*, 2243–2246.

Buzsaki, G., Penttonen, M., Bragin, A., Nadasdy, Z., and Chrobak, J.J. (1995). Possible physiological role of the perforant path-CA1 projection. Hippocampus *5*, 141–146.

Dahl, D., Rueger, D.C., Bignami, A., Weber, K., and Osborn, M. (1981). Vimentin, the 57 000 molecular weight protein of fibroblast filaments, is the major cytoskeletal component in immature glia. Eur. J. Cell Biol. *24*, 191–196.

Dolorfo, C.L., and Amaral, D.G. (1998). Entorhinal cortex of the rat: topographic organization of the cells of origin of the perforant path projection to the dentate gyrus. J. Comp. Neurol. *398*, 25–48.

Dragoi, G., and Buzsaki, G. (2006). Temporal encoding of place sequences by hippocampal cell assemblies. Neuron *50*, 145–157.

Du, F., Eid, T., and Schwarcz, R. (1998). Neuronal damage after the injection of aminooxyacetic acid into the rat entorhinal cortex: a silver impregnation study. Neuroscience *82*, 1165–1178.

Eisch, A.J., Schmued, L.C., and Marshall, J.F. (1998). Characterizing cortical neuron injury with Fluoro-Jade labeling after a neurotoxic regimen of methamphetamine. Synapse *30*, 329–333.

Frank, L.M., Stanley, G.B., and Brown, E.N. (2004). Hippocampal plasticity across multiple days of exposure to novel environments. J. Neurosci. *24*, 7681–7689.

Fuhs, M.C., and Touretzky, D.S. (2006). A spin glass model of path integration in rat medial entorhinal cortex. J. Neurosci. *26*, 4266–4276.

Fyhn, M., Molden, S., Witter, M.P., Moser, E.I., and Moser, M.B. (2004). Spatial representation in the entorhinal cortex. Science *305*, 1258–1264.

Fyhn, M., Hafting, T., Treves, A., Moser, M.B., and Moser, E.I. (2007). Hippocampal remapping and grid realignment in entorhinal cortex. Nature *446*, 190–194.

Gloveli, T., Behr, J., Dugladze, T., Kokaia, Z., Kokaia, M., and Heinemann, U. (2003). Kindling alters entorhinal cortex-hippocampal interaction by increased efficacy of presynaptic GABA(B) autoreceptors in layer III of the entorhinal cortex. Neurobiol. Dis. *13*, 203–212.

Hafting, T., Fyhn, M., Molden, S., Moser, M.B., and Moser, E.I. (2005). Microstructure of a spatial map in the entorhinal cortex. Nature *436*, 801–806.

Hargreaves, E.L., Rao, G., Lee, I., and Knierim, J.J. (2005). Major dissociation between medial and lateral entorhinal input to dorsal hippocampus. Science *308*, 1792–1794.

Harris, K.D., Hirase, H., Leinekugel, X., Henze, D.A., and Buzsaki, G. (2001). Temporal interaction between single spikes and complex spike bursts in hippocampal pyramidal cells. Neuron *32*, 141–149.

Hasselmo, M.E., Bodelon, C., and Wyble, B.P. (2002). A proposed function for hippocampal theta rhythm: separate phases of encoding and retrieval enhance reversal of prior learning. Neural Comput. *14*, 793–817.

Hollup, S.A., Molden, S., Donnett, J.G., Moser, M.B., and Moser, E.I. (2001). Accumulation of hippocampal place fields at the goal location in an annular watermaze task. J. Neurosci. *21*, 1635–1644.

Insausti, R., Herrero, M.T., and Witter, M.P. (1997). Entorhinal cortex of the rat: cytoarchitectonic subdivisions and the origin and distribution of cortical efferents. Hippocampus *7*, 146–183.

Jarsky, T., Roxin, A., Kath, W.L., and Spruston, N. (2005). Conditional dendritic spike propagation following distal synaptic activation of hippocampal CA1 pyramidal neurons. Nat. Neurosci. *8*, 1667–1676.

Jung, M.W., Wiener, S.I., and McNaughton, B.L. (1994). Comparison of spatial firing characteristics of units in dorsal and ventral hippocampus of the rat. J. Neurosci. *14*, 7347–7356.

Khurgel, M., Switzer, R.C., 3rd, Teskey, G.C., Spiller, A.E., Racine, R.J., and Ivy, G.O. (1995). Activation of astrocytes during epileptogenesis in the absence of neuronal degeneration. Neurobiol. Dis. *2*, 23–35.

Lee, I., Yoganarasimha, D., Rao, G., and Knierim, J.J. (2004). Comparison of population coherence of place cells in hippocampal subfields CA1 and CA3. Nature *430*, 456–459.

Leutgeb, S., Leutgeb, J.K., Treves, A., Moser, M.B., and Moser, E.I. (2004). Distinct ensemble codes in hippocampal areas CA3 and CA1. Science *305*, 1295–1298.

Leutgeb, J.K., Leutgeb, S., Treves, A., Meyer, R., Barnes, C.A., McNaughton, B.L., Moser, M.B., and Moser, E.I. (2005a). Progressive transformation of hippocampal neuronal representations in "morphed" environments. Neuron *48*, 345–358.

Leutgeb, S., Leutgeb, J.K., Barnes, C.A., Moser, E.I., McNaughton, B.L., and Moser, M.B. (2005b). Independent codes for spatial and episodic memory in hippocampal neuronal ensembles. Science *309*, 619–623.

Leutgeb, S., Leutgeb, J.K., Moser, M.B., and Moser, E.I. (2005c). Place cells, spatial maps and the population code for memory. Curr. Opin. Neurobiol. *15*, 738–746.

Leutgeb, S., Leutgeb, J.K., Moser, E.I., and Moser, M.B. (2006). Fast rate coding in hippocampal CA3 cell ensembles. Hippocampus *16*, 765–774.

Leutgeb, J.K., Leutgeb, S., Moser, M.B., and Moser, E.I. (2007). Pattern separation in the dentate gyrus and CA3 of the hippocampus. Science *315*, 961–966.

Lever, C., Wills, T., Cacucci, F., Burgess, N., and O'Keefe, J. (2002). Long-term plasticity in hippocampal place-cell representation of environmental geometry. Nature *416*, 90–94.

Li, X.G., Somogyi, P., Ylinen, A., and Buzsaki, G. (1994). The hippocampal CA3 network: an in vivo intracellular labeling study. J. Comp. Neurol. *339*, 181–208.

Marr, D. (1971). Simple memory: a theory for archicortex. Philos. Trans. R. Soc. Lond. B Biol. Sci. *262*, 23–81.

McNaughton, B.L., and Morris, R.G.M. (1987). Hippocampal synaptic enhancement and information storage within a distributed memory system. Trends Neurosci. *10*, 408–415.

McNaughton, B.L., Barnes, C.A., Meltzer, J., and Sutherland, R.J. (1989). Hippocampal granule cells are necessary for normal spatial learning but not for spatially-selective pyramidal cell discharge. Exp. Brain Res. *76*, 485–496.

McNaughton, B.L., Battaglia, F.P., Jensen, O., Moser, E.I., and Moser, M.-B. (2006). Path-integration and the neural basis of the 'cognitive map'. Nat. Rev. Neurosci. *7*, 663–678.

Mizumori, S.J., McNaughton, B.L., Barnes, C.A., and Fox, K.B. (1989). Preserved spatial coding in hippocampal CA1 pyramidal cells during reversible suppression of CA3c output: evidence for pattern completion in hippocampus. J. Neurosci. *9*, 3915–3928.

Mullen, R.J., Buck, C.R., and Smith, A.M. (1992). NeuN, a neuronal specific nuclear protein in vertebrates. Development *116*, 201–211.

Muller, R.U., and Kubie, J.L. (1989). The firing of hippocampal place cells predicts the future position of freely moving rats. J. Neurosci. *9*, 4101–4110.

Muller, R.U., Kubie, J.L., and Ranck, J.B., Jr. (1987). Spatial firing patterns of hippocampal complex-spike cells in a fixed environment. J. Neurosci. *7*, 1935–1950.

Naber, P.A., Witter, M.P., and Lopez da Silva, F.H. (1999). Perirhinal cortex input to the hippocampus in the rat: evidence for parallel pathways, both direct and indirect. A combined physiological and anatomical study. Eur. J. Neurosci. *11*, 4119–4133.

Naber, P.A., Lopes da Silva, F.H., and Witter, M.P. (2001). Reciprocal connections between the entorhinal cortex and hippocampal fields CA1 and the subiculum are in register with the projections from CA1 to the subiculum. Hippocampus *11*, 99–104.

Nakazawa, K., Quirk, M.C., Chitwood, R.A., Watanabe, M., Yeckel, M.F., Sun, L.D., Kato, A., Carr, C.A., Johnston, D., Wilson, M.A., and Tonegawa, S. (2002). Requirement for hippocampal CA3 NMDA receptors in associative memory recall. Science *297*, 211–218.

Nakazawa, K., Sun, L.D., Quirk, M.C., Rondi-Reig, L., Wilson, M.A., and Tonegawa, S. (2003). Hippocampal CA3 NMDA receptors are crucial for memory acquisition of one-time experience. Neuron *38*, 305–315.

O'Keefe, J., and Dostrovsky, J. (1971). The hippocampus as a spatial map. Preliminary evidence from unit activity in the freely-moving rat. Brain Res. *34*, 171–175.

O'Keefe, J., and Burgess, N. (2005). Dual phase and rate coding in hippocampal place cells: theoretical significance and relationship to entorhinal grid cells. Hippocampus *15*, 853–866.

Remondes, M., and Schuman, E.M. (2002). Direct cortical input modulates plasticity and spiking in CA1 pyramidal neurons. Nature *416*, 736–740.

Remondes, M., and Schuman, E.M. (2004). Role for a cortical input to hippocampal area CA1 in the consolidation of a long-term memory. Nature *431*, 699–703.

Sargolini, F., Fyhn, M., Hafting, T., McNaughton, B.L., Witter, M.P., Moser, M.B., and Moser, E.I. (2006). Conjunctive representation of position, direction, and velocity in entorhinal cortex. Science *312*, 758–762.

Schmitzer-Torbert, N., Jackson, J., Henze, D., Harris, K., and Redish, A.D. (2005). Quantitative measures of cluster quality for use in extracellular recordings. Neuroscience *131*, 1–11.

Schmued, L.C., and Hopkins, K.J. (2000). Fluoro-Jade B: a high affinity fluorescent marker for the localization of neuronal degeneration. Brain Res. *874*, 123–130.

Schmued, L.C., Albertson, C., and Slikker, W., Jr. (1997). Fluoro-Jade: a novel fluorochrome for the sensitive and reliable histochemical localization of neuronal degeneration. Brain Res. *751*, 37–46.

Shah, M.M., Anderson, A.E., Leung, V., Lin, X., and Johnston, D. (2004). Seizure-induced plasticity of h channels in entorhinal cortical layer III pyramidal neurons. Neuron *44*, 495–508.

Shao, L.R., and Dudek, F.E. (2004). Increased excitatory synaptic activity and local connectivity of hippocampal CA1 pyramidal cells in rats with kainate-induced epilepsy. J. Neurophysiol. *92*, 1366–1373.

Siddiqui, A.H., and Joseph, S.A. (2005). CA3 axonal sprouting in kainate-induced chronic epilepsy. Brain Res. *1066*, 129–146.

Skaggs, W.E., McNaughton, B.L., Gothard, K.M., and Markus, E.J. (1993). Advances in Neural Information Processing Systems, Volume 5 (San Mateo, CA: Morgan Kaufmann).

Solstad, T., Moser, E.I., and Einevoll, G.T. (2006). From grid cells to place cells: a mathematical model. Hippocampus *16*, 1026–1031.

Steffenach, H.A., Sloviter, R.S., Moser, E.I., and Moser, M.B. (2002). Impaired retention of spatial memory after transection of longitudinally oriented axons of hippocampal CA3 pyramidal cells. Proc. Natl. Acad. Sci. USA *99*, 3194–3198.

Steward, O. (1976). Topographic organization of th eprojections from the entorhinal area to the hippocampal formation of the rat. J. Comp. Neurol. *167*, 285–314.

Swanson, L.W., and Köhler, C. (1986). Anatomical evidence for direct projections from the entorhinal area to the entire cortical mantle in the rat. J. Neurosci. *6*, 3010–3023.

Taube, J.S., Muller, R.U., and Ranck, J.B., Jr. (1990). Head-direction cells recorded from the postsubiculum in freely moving rats. II. Effects of environmental manipulations. J. Neurosci. *10*, 436–447.

Treves, A., and Rolls, E.T. (1991). What determines the capacity of autoassociative memories in the brain. Network *2*, 371–397.

Vazdarjanova, A., and Guzowski, J.F. (2004). Differences in hippocampal neuronal population responses to modifications of an environmental context: evidence for distinct, yet complementary, functions of CA3 and CA1 ensembles. J. Neurosci. *24*, 6489–6496.

Wilson, M.A., and McNaughton, B.L. (1993). Dynamics of the hippocampal ensemble code for space. Science *261*, 1055–1058.

Witter, M.P., and Amaral, D.G. (2004). Hippocampal formation. In The Rat Nervous System, Third Edition, G. Paxinos, ed. (San Diego, CA: Academic Press), pp. 637–703, Chapter 21.

Witter, M.P., Groenewegen, H.J., Lopes da Silva, F.H., and Lohman, A.H. (1989). Functional organization of the extrinsic and intrinsic circuitry of the parahippocampal region. Prog. Neurobiol. *33*, 161–253.

Wouterlood, F.G., and Groenewegen, H.J. (1991). The Phaseolus vulgaris-leucoagglutinin tracing technique for the study of neuronal connections. Prog. Histochem. Cytochem. *22*, 1–78.

Wu, H.Q., and Schwarcz, R. (1998). Focal microinjection of gamma-acetylenic GABA into the rat entorhinal cortex: behavioral and electroencephalographic abnormalities and preferential neuron loss in layer III. Exp. Neurol. *153*, 203–213.